Model Calibration Methods for Phase Diagram Determination

Brian J. Reardon[a] *and Marius Stan*[b]

[a]Los Alamos National Laboratory, Engineering Sciences and Applications Division, Los Alamos, NM, USA
[b] Los Alamos National Laboratory Materials Science and Technology Division, Los Alamos, NM USA
E-mail: breardon@lanl.gov, mastan@lanl.gov

Abstract: A heuristic optimization methodology based on a Genetic Algorithm is presented with the goal to help researchers decide on the optimal set of thermodynamic data and models to use to accurately model phase diagrams and their associated uncertainty. This approach accounts for the errors associated with reported data and how reliable the researcher believes the model to be. Additionally, the results of the Genetic Algorithm provides guidance as to which experiments are needed to enhance the reliability of the dataset and is ideally suited for parameter optimization and sensitivity analysis. Applications include the UO_2-PuO_2 and UO_2-BeO systems.

Keywords: Genetic Algorithms, model calibration, uncertainty

1.0 INTRODUCTION

Finding an optimal model by fitting thermodynamic data is a difficult problem in materials science due to the large uncertainty associated with the experimental or calculated data sets that are used as input. This situation is most prevalent in the case of the calculation of phase diagrams [1] where the solidus and liquidus boundaries are highly uncertain [2] due to limitations in the accuracy of temperature measurements, limitations in determining the phase transition boundaries, and the potential for off-stoichiometric compositions at high temperature. In spite of all of these uncertainties or perhaps because of them, one rarely finds the uncertainty bounds reported with the phase diagram.

One could address this problem in several ways, each having a number of limitations. The first would be to simply accept a particular set of thermodynamic data as fact and use these values to calculate phase equilibrium curves. This approach ignores all the data available in other thermodynamic assessments as well as any phase diagram data. It also assumes that the selected data set is the best available. The second approach would be to take an average of all the known thermodynamic data sets. It assumes that all the thermodynamic data is equal in quality and thus only an average is necessary. This approach also ignores the available phase diagram data. Another option is to fit the solidus and liquidus equations to the known phase diagram data. The starting point of the optimization heavily influences this approach. Furthermore, it essentially ignores the experimental thermodynamic data once the optimization has initiated. The method proposed in this work uses a Genetic Algorithm to incorporate all the data and its associated uncertainties into an optimal fit of what is known.

The scientific literature is notably bereft of papers dedicated to the analysis of the uncertainties associated with equilibrium phase diagrams. A classical approach, based on the "spread of mistakes" formalism, is presented in [3] while in [4] a way of extracting the maximum information from a minimal set of experimental data is investigated. Bayesian based methods have been used to produce self-consistent thermodynamic data sets for binary

Sensitivity Analysis of Model Output
Kenneth M. Hanson and François M. Hemez, eds.
Los Alamos National Laboratory, 2005; http://library.lanl.gov/

[5] or multi-component [6-8] systems. All papers emphasize the importance of starting with a reliable, self-consistent thermodynamic data set and draw the reader's attention to the propagation of the errors in the input parameters during the calculation process.

This work demonstrates that modern heuristic optimization techniques such as Genetic Algorithms offer a viable way of relating models to the data in the face of large uncertainties both on the model parameters and the training data. To illustrate the utility of this approach the solidus and liquidus boundaries of the UO_2-PuO_2 and UO_2-BeO systems have been selected. The parameter optimization was performed for each binary system given some information about the solidus and liquidus boundaries, the heats of melting, ΔH^M, and the melting temperatures, T^M.

1.1 Genetic Algorithms

Genetic Algorithms are heuristic optimization techniques that borrow heavily from the ideas of Darwinian evolution. Using evolution as an optimization tool was first proposed by Holland [9] and ever since has spurred a large amount of interest [10]. A genetic algorithm borrows the three main constructs of Darwinian evolution (selection, crossover, and mutation) to evolve a set of parameter vectors towards an optimal solution.

In the parlance of the GA community, the set of parameter vectors is a population. Each member of the population is evaluated to determine how well it solves the problem at hand, i.e. to determine their fitness. The most fit members are selected with a probability proportional to their fitness and allowed to exchange genetic information with other members and thus create the next population which usually has a higher average fitness than the parent population.

As a population based optimization method, the GA is ideally suited to handle the various forms of uncertainty found in this problem with a minimum of assumption about what the uncertainty should look like. The first form of uncertainty lays in the phase diagram data itself. Figure 1 shows the experimental solidus and liquidus data from three different sources. In this work the GA must fit a model through this data. The error bars on both the composition and temperature can be interpreted as nothing more than random intervals and thus there is no way to discern any type of uncertainty distribution on the intervals. Uncertainty in the experimental data relaxes the constraints on the optimal parameter values and forces us to identify a range of parameter values that provide a range of calculated values that lay within the experimental uncertainty. Thus, this problem is under specified. Previous work [11] has shown that a selection operator that uses a fuzzy logic-weighting scheme effectively handles optimization scenarios such as this where there are potentially a very large number of solutions all of equal fitness and plausibility.

A fuzzy logic-weighting scheme [12] looks at all the objective values of a particular member and rescales them to a value between 0 and 1. 0 if the value is the worst of the population. 1 if it falls within the experimental uncertainty. Once the objectives have been scaled, the average is taken over all objectives and that single number is the fitness for the member in the population.

Using the fuzzy logic weighting scheme, the GA is run until all the members of the population reach a fitness of 1 or at least reach a state of equilibrium where there is no more improvement. When this state is reached, the members of the final population are used to determine the uncertainty bounds on the model parameters. The population of final

parameters can then be used to bound output of the model and show where the model is most uncertain and in need of more data.

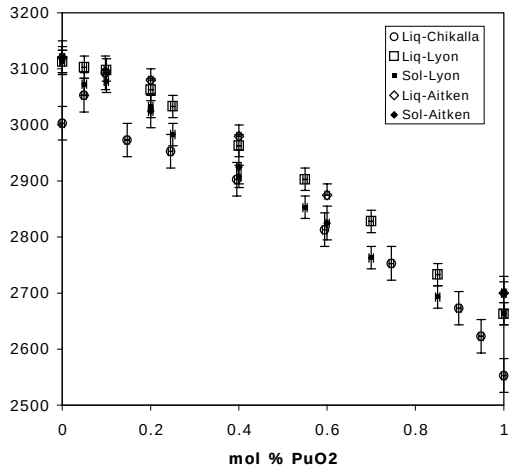

Figure 1. The experimental solidus and liquidus data for the UO_2-PuO_2 system from Chikalla, Lyon and Baily, and Aitken and Evans.

Another form of uncertainty lays in the search ranges for many of the input model parameters being optimized. For some models, the input parameters are in fact experimentally accessible values which themselves contain a large amount of uncertainty. Such parameters would be the melting points of the starting compositions (UO_2, PuO_2, BeO) as well as their heats of melting. Other models are purely empirical and were developed by various authors to fit their particular data sets. The empirical parameters have no physical meaning. If such a model is to be fit to a different set of data, the published parameters could be used as a starting point. Unfortunately, the parameters in question are rarely published with any sort of assessment of uncertainty and one must then make an educated guess as to what a reasonable search range would be.

There are a number of advantages to using a GA in this problem over other calibration approaches. First, a multi-objective GA tends to be robust enough to identify distributions of solutions. These distributions are often multi-modal and thus have shapes not easily captured by traditional calibration routines. Second, the GA requires no preconceived assumptions about the uncertainty distributions on the objective data or the parameter values. However, if desired, assumed distributions are easily incorporated. Third, and probably most importantly, the GA incorporates all the known data into its search. For example, the known phase diagram data defines the objectives and the spread of the known thermodynamic data defines the search space.

2. PROCEDURE

This work will address how well 5 different models fit and explain 3 different data sets and combinations thereof all of which are supposed to describe the solidus and liquidus curves of the UO_2-PuO_2 phase diagram as shown in Figure 1.

The first data set is that of Chikalla [13] which only shows a liquidus curve. The liquidus curve behaves as one would expect for an ideal solid solution except for the PuO_2 values of

of 5 and 10 wt%. The data also shows significant scatter in liquidus temperature at all compositions but especially at 75 wt% PuO_2. Note that there is no scatter displayed or reported in the composition (x axis). It was presumed by the authors that the composition was known exactly even though it is common knowledge that composition can drift due to changes in oxygen partial pressure and vaporization of the components. It is also worth nothing that Chikalla, admits later in his paper that the liquidus must be much lower in temperature throughout the entire PuO_2 composition range due to thermodynamic considerations and known melting points and heats of melting. However, other authors believe the liquidus to be much higher.

The second data set is from Lyon and Baily [14] and is generally considered to be a much more well-behaved and thus reliable experimental determination of both the solidus and liquidus of the UO_2-PuO_2 phase diagram. Lyon and Baily also compute the solidus and liquidus curves using the Ideal Solutions laws and generally show a much better fit than Chikalla did in his study. Like Chikalla, however, uncertainties were never properly accounted for in this study. For example, the composition is still assumed to be known exactly and in many cases, especially at very small and very large PuO_2 compositions, the temperature error bars of the solidus and curves overlap significantly. Both Chikalla and Lyon also use the generally accepted Ideal Solution model to calculate the solidus and liquidus curves. While this model is known to be quite accurate and extendable to other systems because it is based on first principles, it has a down fall when it comes to fitting phase diagram data. Namely, phase diagram data is usually collected by changing the composition (x) and measuring the temperature of the phase transitions (y) whereas the Ideal Solution model is the inverse. It assumes a temperature and calculates the composition of the solidus and liquidus. This inversion presents somewhat of a problem in the context of fitting a model to the data since the effect of experimental uncertainties cannot be directly propagated through the optimizer.

The third data set is that of Aitken and Evans [15, 16]. Aitken and Evans, like Lyon and Bailly, experimentally determine the solidus and liquidus of the UO_2-PuO_2 system by varying the composition and measuring the temperature at which the solidus and liquidus are observed. Aitken and Evans differ from Lyon and Baily and also Chikalla by attempting to fit the observed solidus and liquidus data with different polynomial forms. The advantage of this approach is that the polynomial forms, like the data, provide a measure of temperature as a function of composition and thus are more amenable to proper uncertainty propagation. The downside of this approach is obvious. Namely, the polynomials are only applicable to the phase diagrams at hand and their parameters cannot be used in a predictive fashion for other thermodynamic studies.

2.1 Model Descriptions

2.1.1 Model 1. Ideal Solid Solution Law

The UO_2-PuO_2 system shows complete solubility of the two components in the solid phase [17]. The liquidus (x^{Liq}) and solidus (x^{Sol}) mole fractions for each fixed temperature (T) can be approximated [18, 19] by:

$$x^{Liq}(T) = \frac{1 - \exp\left(\frac{\Delta H^{M}_{UO_2}}{R}\left(\frac{1}{T} - \frac{1}{T^{M}_{UO_2}}\right)\right)}{\exp\left(\frac{\Delta H^{M}_{PuO_2}}{R}\left(\frac{1}{T} - \frac{1}{T^{M}_{PuO_2}}\right)\right) - \exp\left(\frac{\Delta H^{M}_{UO_2}}{R}\left(\frac{1}{T} - \frac{1}{T^{M}_{UO_2}}\right)\right)} \quad (1)$$

and

$$x^{Sol}(T) = x^{Liq}(T) \cdot \exp\left(\frac{\Delta H^{M}_{PuO_2}}{R}\left(\frac{1}{T} - \frac{1}{T^{M}_{PuO_2}}\right)\right) \quad (2)$$

Where R is the gas constant (8.314 J/mol K).

The values of the input parameters for the UO_2-PuO_2 system are scattered [13, 15, 20-22], leading to large uncertainty bounds, as shown in Table I. The goal of our work is to further refine the values of the input parameters using the GA given known experimental data on the solidus and liquidus positions (Figure 1). Thus, the optimization proceeds as follows: First, the search range for each parameter is defined for the GA based on the accepted uncertainty or variation in the published parameter values. Second, the GA evolves the parameter values based on how well the values generate solidus and liquidus curves, which match the available experimental data – taking into account the uncertainties of the experimental solidus and liquidus curves. For this study the initial uncertainty in concentration was assumed to be 0.005 and the uncertainty in the liquidus and solidus temperatures was 55K and 35K respectively. Once the range of parameter values is optimized, values from this range are placed in the forward model. This results in fuzzy bands that define the position of the curves which are most self consistent given all data and the underlying model. Of particular importance to note is that the total uncertainty in model parameter values as well as the solidus and liquidus curves decreases by using this method approach.

Table I. The Upper and Lower Limits of the Variable Search Space [13, 15, 20-22].

Variable	Units	Lower value	Upper value
ΔH^{M}_{UO2}	kJ/mol	25	125
ΔH^{M}_{BeO}	kJ/mol	42	125
ΔH^{M}_{PuO2}	kJ/mol	25	100
T^{M}_{UO2}	K	3000	3200
T^{M}_{BeO}	K	2700	2900
T^{M}_{PuO2}	K	2600	2800

2.1.2 Model 2: polynomial in (x)

Adamson et al. (in Aitken) recommend the following model for the solidus and liquidus curves of UO_2-PuO_2

$$T_s(K) = a_s + b_s x + c_s x^2 + d_s x^3$$
$$T_l(K) = a_l + b_l x + c_l x^2 \quad (3)$$

where a_s = 3120, b_s=-655.3, c_s=336.4, d_s=-99.9 and a_l=3120, b_l=-388.1, c_l=-30.4. Note that the polynomial is in x as opposed to T as in Model 1.

2.1.3 Model 3; polynomial in (x)

Lyon and Baily recommend the following model for the solidus and liquidus curves of UO_2-PuO_2

$$T_s(K) = a_s + b_s x + c_s x^2$$
$$T_l(K) = a_l + b_l x + c_l x^2 \quad (4)$$

where a_s = 3113.15, b_s=-5.41395, c_s=7.4639e-3 and a_l=3113.15, b_l=-3.2166, c_l=-1.448518e-3.

2.1.4 Model 4: polynomial in (x)

Komatsu et al. (in Aitken) recommend the following model for the solidus and liquidus curves of UO_2-PuO_2

$$T_s(K) = T_{MUO_2} / \left(1 + b_s x + c_s x^2\right)$$
$$T_l(K) = T_{MUO_2} / \left(1 + b_l x + c_l x^2\right) \quad (5)$$

where b_s=0.1811, c_s=-0.011 and b_l=0.1068, c_l=0.06316.

2.1.5 Model 5: standard thermodynamic in T but extended to other phase diagram data

Another advantage of using a GA with a fuzzy logic selection method is that different types of objective functions can be easily combined. In this exercise the objective goals of Model 1 are combined with the objective goals and data of a thermodynamic model of the eutectic UO_2-BeO system. To optimize the UO_2-BeO system, a similar procedure as for the UO_2-PuO_2 system was employed. For this type of diagram the equilibrium lines are defined by:

$$x^{Liq}_{UO_2+Liq}(T) = 1 - \exp\left(\left(\frac{-\Delta H^M_{UO_2}}{RT}\right)\ln\left(\frac{T^M_{UO_2}}{T}\right)\right) \quad (6)$$

and

$$x^{Liq}_{Liq+BeO}(T) = \exp\left(\left(\frac{-\Delta H^M_{BeO}}{RT}\right)\ln\left(\frac{T^M_{BeO}}{T}\right)\right) \quad (7)$$

The values of the melting enthalpy and temperature were obtained from the literature and are displayed in Table I. Note that the both Model 1 and the eutectic model require thermodynamic values for UO_2. Thus, by incorporating this model into the optimization scheme, the potential thermodynamic values for UO_2 are constrained. Unfortunately, the thermodynamic values for BeO are also required. The reader should take heart, however, that this process of combining objectives, models and data allows one to obtain thermodynamically self consistent values for the basic properties of the constituent compositions – something that is typically very hard to do using other uncertainty propagation methods. The UO_2-BeO phase diagram [23] shows a eutectic point at T = 2450 K and BeO mole fraction x = 0.68. Namely x_{BeO} = 0.68±0.05 (Figure 2). For this study the uncertainty in

the liquidus concentration was again 0.05 and the temperature uncertainty was 40K. In the model, the eutectic composition is defined as that point in which the curves calculated from Eq. (6) and Eq. (7) intersect. This point also defines the calculated eutectic temperature. While the eutectic temperature is known experimentally, there is no information gain in comparing it to the calculated value since the calculated value is determined by the calculated value of the eutectic composition.

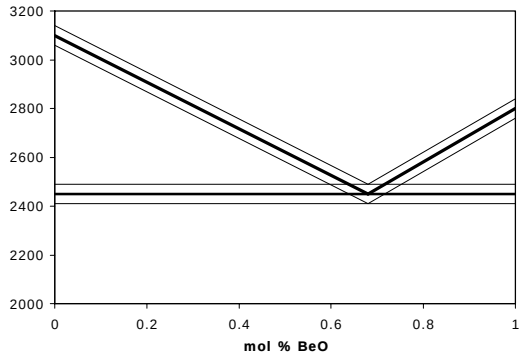

Figure 2. The experimental eutectic point for the UO_2-BeO system at 0.68 mol% BeO.

3. RESULTS

Table II shows the results of the optimization with each model described previously and when using different data sets. The table shows the model used, data set used, number of solutions found and the fitness of said solutions. The maximum possible fitness is 1.0 and would indicate that all the calculated values fall within the experimental uncertainty of the data.

3.1 Model 1

Tests 1-10 used model 1 with the listed data sets. The difference between tests 1-5 and 6-10 is the stated uncertainty of the composition values. In tests 1-5 the uncertainty is 0.005 whereas in tests 6-10 it is 0.05. Note that experimentally the uncertainty in composition is very small (0.005 is a reasonable number) whereas the uncertainty in temperature is much higher. Unfortunately, Model 1 is written as a function of temperature, not composition. Thus when the model optimized against the raw data, it rarely falls within the experimental uncertainty of x. The net result of this fact for tests 1-5 is that the apparent fitness of the optimal solutions is very low. To get around this problem and find a large set of solutions that actually pass through the known uncertainty bounds of the experimental data, the uncertainty in composition was expanded based on the degree to which the uncertainty in x would intersect uncertainties in temperature of neighboring compositions. The final assessment of this 'graphically driven' as opposed to data driven uncertainty was an interval of size ±0.05. Tests 6-10 show the results of using this 'graphically driven' uncertainty in x. Note that all of the fitnesses increase as would be expected but most notably, a total of 394 solutions were found that perfectly match the experimental data of Lyon and Baily.

These results indicate that Lyon and Baily's experimental data is most consistent with the Ideal Solution assumptions of Model 1. Further it correctly identifies Chikalla's data as being the most suspect.

Table II. The results of optimizing each model against the available data sets. C: Chikalla, L: Lyon and Baily, and A: Aitken and Evans.

Test	Model	Data Sets	# Solutions	Fitness
1	1a	L	1	0.949274
2	1a	A	1	0.976892
3	1a	C	1	0.84066
4	1a	L+A	1	0.928932
5	1a	L+A+C	1	0.790519
6	1b	L	394	1
7	1b	A	1	0.989953
8	1b	C	1	0.887064
9	1b	L+A	1	0.99024
10	1b	L+A+C	1	0.874315
11	2	L	5	0.998358
12	2	A	377	1
13	2	C	1	0.9591
14	2	L+A	14	0.995911
15	2	L+A+C	1	0.941159
16	3	L	145	0.998775
17	3	A	291	1
18	3	C	502	1
19	3	L+A	82	0.993154
20	3	L+A+C	2	0.930555
21	4	L	3	0.983283
22	4	A	1	0.993808
23	4	C	449	0.960122
24	4	L+A	1	0.982623
25	4	L+A+C	1	0.920988
26	5a	L	11	0.974211
27	5a	A	322	0.981022
28	5a	C	105	0.899736
29	5a	L+A	1	0.963978
30	5a	L+A+C	7	0.894648
31	5b	L	308	0.999815
32	5b	A	255	1
33	5b	C	395	0.933822
34	5b	L+A	43	0.995135
35	5b	L+A+C	127	0.930271

3.2 Models 2-4

Models 2, 3, and 4 are polynomial functions originally designed to fit specific data sets. From the results of Table 1I this fact is clear since some models find a large number of highly fit solutions for one set of data and not the others. It should also be pointed out that since the polynomials are functions of composition, they are able to more accurately account for the uncertainty in the temperature data. Thus, they give the illusion of being better fit models than the thermodynamically based Model 1. Unfortunately, though these models appear to fit

much of the data very well they are in no way extensible to other phase systems. In other words where the melting points and heats of melting optimized in Model 1 can then be used to estimate the behavior other phase systems, the parameters of Models 2-4 cannot.

3.3 Model 5

Like Model 1, two values were used for the uncertainties in composition. Namely, ±0.005 for Tests 26-30 and ±0.05 for Tests 31-35. Also, as was the case for Model 1, the larger uncertainties in composition faired better in the optimization. This is evidenced by the higher fitness values and number of solutions for all of the data sets optimized against. The most notable difference between the output of Models 1 and 5 is shown in Figure 3, however. Model 1 had to optimize the values for the melting point and heats of melting of UO_2 and PuO_2 whereas Model 5 also had to optimized the same values for BeO. Since the values for UO_2 were needed in both the Ideal solution model of UO_2-PuO_2 and the simple eutectic model of UO_2-BeO, the ultimate optimal values were much more constrained in Model 5. Figure 3 shows the optimal melting point and heat of formation for UO_2 from Models 1 (circle) and Model 5 (square). Note that since UO_2 was much more constrained in Model 5, only one viable solution was found.

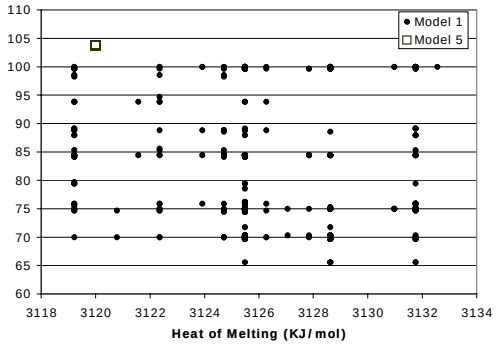

Figure 3. The final solution sets for the heats of melting and the melting points of UO_2 determined through the optimization of Model 1 (circle) and Model 5 (square).

4. CONCLUSIONS

The use of a Genetic Algorithm allows for incorporating uncertain data sets, both large and small, in an efficient and meaningful way. This process then leads to the optimization of the parameters of proposed models and the assessment of the overall predictive credibility of said models. Specifically, this work determines the degree of uncertainty on the phase boundaries of the UO_2-PuO_2 and UO_2-BeO systems by taking into account the available phase boundary data, the accepted models of the phase boundaries, and the thermodynamic data used in those models. The net result was an overall reduction in uncertainty of the values of the thermodynamic data as well as the phase boundary positions in a way that is internally self-consistent. The use of modern heuristic optimizers such as genetic algorithms was crucial to this work since they are both robust and require no assumptions about the forms of the uncertainty distributions.

5. REFERENCES

1. M. Stan, Phase Diagram Calculations in Materials Processing, *Control and Optimization in Minerals, Metals and Materials Processing*. 1999, Met. Soc.: Montreal.

2. M.I. Baskes, and M. Stan, An atomistic study of solid/liquid interfaces and phase equilibrium in binary systems. *Met. Trans. A*: Physical Metallurgy and Materials Science, 2003. **34**: p. 435-439.
3. D.V. Malakhov, Confidence intervals of calculated phase boundaries. *Calphad-Computer Coupling of Phase Diagrams and Thermochemistry*, 1997. **21**(3): p. 391-400.
4. E. Konigsberger, Improvement of Excess Parameters from Thermodynamic and Phase-Diagram Data by a Sequential Bayes Algorithm. *Calphad-Computer Coupling of Phase Diagrams and Thermochemistry*, 1991. **15**(1): p. 69-78.
5. J. Acker, and K. Bohmhammel, Optimization of thermodynamic data of the Ni-Si system. *Thermochimica Acta*, 1999. **337**(1-2): p. 187-193.
6. N.D. Chatterjee, et al., The Bayesian approach to an internally consistent thermodynamic database: theory, database, and generation of phase diagrams. *Contributions to Mineralogy and Petrology*, 1998. **133**(1-2): p. 149-168.
7. N.D. Chatterjee, K. Miller, and W. Olbricht, Bayes Estimation - a Novel-Approach to Derivation of Internally Consistent Thermodynamic Data for Minerals, Their Uncertainties, and Correlations .2. Application. *Physics and Chemistry of Minerals*, 1994. **21**(1-2): p. 50-62.
8. W. Olbricht, N.D. Chatterjee, and K. Miller, Bayes Estimation - a Novel-Approach to Derivation of Internally Consistent Thermodynamic Data for Minerals, Their Uncertainties, and Correlations .1. Theory. *Physics and Chemistry of Minerals*, 1994. **21**(1-2): p. 36-49.
9. J.H. Holland, Adaptation in Natural and Artificial systems. Complex adaptive systems. 1992, Cambridge: MIT Press. 211 p. : ill. ; 24 cm.
10. D.E. Goldberg, *Genetic Algorithms in Search, Optimization, and Machine Learning*. 1989, Reading: Addison-Wesley Pub. Co. 412 p. : ill. ; 25 cm.
11. B.J. Reardon, Inversion of micromechanical powder consolidation and sintering models using Bayesian inference and genetic algorithms. *Modelling and Simulation in Materials Science and Engineering*, 1999. **7**(6): p. 1061-1081.
12. B.J. Reardon, Fuzzy logic versus niched Pareto multiobjective genetic algorithm optimization. *Modelling and Simulation in Materials Science and Engineering*, 1998. **6**(6): p. 717-734.
13. T.D. Chikalla, Melting Behavior in the System UO2-PuO2. *Journal of the American Ceramic Society*, 1963. **46**(7): p. 323-328.
14. W.L. Lyon, and W.E. Baily, Solid-Liquid Phase Diagram for UO2-PuO2 System. *Journal of Nuclear Materials*, 1967. **22**(3): p. 332.
15. E.A. Aitken, and S.K. Evans, A Thermodynamic Data Program Involving Plutonia and Urania at High Temperatures, in Quarterly Report. 1968, General Electric: Pleasanton, California.
16. M.G. Adamson, E.A. Aitken, and R.W. Caputi, Experimental and Thermodynamic Evaluation of the Melting Behavior of Irradiated Oxide Fuels. *Journal of Nuclear Materials*, 1985. **130**(EB): p. 349-365.
17. L.F. Epstein, Ideal Solution Behavior and Heats of Fusion from UO2-PuO2 Phase Diagram. *Journal of Nuclear Materials*, 1967. **22**(3): p. 340-349.
18. L.F. Epstein, and W.H. Howland, Binary Mixtures of UO2 and Other Oxides. *Journal of the American Ceramic Society*, 1953. **36**(10): p. 334-335.
19. H. Seltz, Thermodynamics of Solid Solutions: I. Perfect Solutions. *Journal of the American Chemical Society*, 1934. **56**: p. 307-311.
20. M.G. Adamson, E.A. Aitken, and R.W. Caputi, Experimental and Thermodynamic Evaluation of the Melting Behavior of Irradiated Oxide Fuels. *Journal of Nuclear Materials*, 1985. **130**(EB): p. 349-365.
21. M.H. Rand, et al., Thermodynamic Properties of the Urania Phase. *Revue Internationale Des Hautes Temperatures Et Des Refractaires*, 1978. **15**(4): p. 355-365.
22. W.L. Lyon, and W.E. Baily, Solid-Liquid Phase Diagram for UO2-PuO2 System. *Journal of Nuclear Materials*, 1967. **22**(3): p. 332.
23. P.P. Budnikov, S.G. Tresvyatski, and V.I. Kushakovsky. in Proc. 2nd U. N. Intern. Conf. Peaceful Uses At. Energy. 1958. Geneva.